NASA/TM—2011–215977

Flight Test Results from the Rake Airflow Gage Experiment on the F-15B Airplane

Michael A. Frederick and Nalin A. Ratnayake

Dryden Flight Research Center, Edwards, California

September 2011

NASA STI Program ... in Profile

Since its founding, NASA has been dedicated to the advancement of aeronautics and space science. The NASA scientific and technical information (STI) program plays a key part in helping NASA maintain this important role.

The NASA STI program operates under the auspices of the Agency Chief Information Officer. It collects, organizes, provides for archiving, and disseminates NASA's STI. The NASA STI program provides access to the NASA Aeronautics and Space Database and its public interface, the NASA Technical Report Server, thus providing one of the largest collections of aeronautical and space science STI in the world. Results are published in both non-NASA channels and by NASA in the NASA STI Report Series, which includes the following report types:

- TECHNICAL PUBLICATION. Reports of completed research or a major significant phase of research that present the results of NASA Programs and include extensive data or theoretical analysis. Includes compilations of significant scientific and technical data and information deemed to be of continuing reference value. NASA counterpart of peer-reviewed formal professional papers but has less stringent limitations on manuscript length and extent of graphic presentations.

- TECHNICAL MEMORANDUM. Scientific and technical findings that are preliminary or of specialized interest, e.g., quick release reports, working papers, and bibliographies that contain minimal annotation. Does not contain extensive analysis.

- CONTRACTOR REPORT. Scientific and technical findings by NASA-sponsored contractors and grantees.

- CONFERENCE PUBLICATION. Collected papers from scientific and technical conferences, symposia, seminars, or other meetings sponsored or co-sponsored by NASA.

- SPECIAL PUBLICATION. Scientific, technical, or historical information from NASA programs, projects, and missions, often concerned with subjects having substantial public interest.

- TECHNICAL TRANSLATION. English-language translations of foreign scientific and technical material pertinent to NASA's mission.

Specialized services also include organizing and publishing research results, distributing specialized research announcements and feeds, providing help desk and personal search support, and enabling data exchange services.

For more information about the NASA STI program, see the following:

- Access the NASA STI program home page at *http://www.sti.nasa.gov*

- E-mail your question via the Internet to help@sti.nasa.gov

- Fax your question to the NASA STI Help Desk at 443-757-5803

- Phone the NASA STI Help Desk at 443-757-5802

- Write to:
  NASA STI Help Desk
  NASA Center for AeroSpace Information
  7115 Standard Drive
  Hanover, MD 21076-1320

NASA/TM—2011–215977

Flight Test Results from the Rake Airflow Gage Experiment on the F-15B Airplane

Michael A. Frederick and Nalin A. Ratnayake

Dryden Flight Research Center, Edwards, California

National Aeronautics and
Space Administration

Dryden Flight Research Center
Edwards, CA 93523-0273

September 2011

Available from:

NASA Center for AeroSpace Information
7115 Standard Drive
Hanover, MD 21076-1320
443-757-5802

Abstract

The Rake Airflow Gage Experiment involves a flow-field survey rake that was flown on the Propulsion Flight Test Fixture at the National Aeronautics and Space Adminstration Dryden Flight Research Center using the Dryden F-15B research test bed airplane. The objective of this flight test was to ascertain the flow-field angularity, local Mach number profile, total pressure distortion, and dynamic pressure at the aerodynamic interface plane of the Channeled Centerbody Inlet Experiment. This new mixed-compression, supersonic inlet is planned for flight test in the near term. Knowledge of the flow-field characteristics at this location underneath the airplane is essential to flight-test planning and computational modeling of the new inlet, and it is also applicable for future propulsion systems research that may use the Propulsion Flight Test Fixture. This report describes the flight-test preparation and execution, and the local flow-field properties calculated from pressure measurements of the rake. Data from the two Rake Airflow Gage Experiment research flights demonstrate that the F-15B airplane, flying at a free-stream Mach number of 1.65 and a pressure altitude of 40,000 ft, would achieve the desired local Mach number for the future inlet flight test. Interface plane distortion levels of 2 percent and a local angle of attack of –2° were observed at this condition. Alternative flight conditions for future testing and an exploration of certain anomalous data also are provided.

Nomenclature

CCIE	Channeled Centerbody Inlet Experiment
CDE	Cone Drag Experiment
LMI	Local Mach Investigation
m	mean flow quantity
M_∞	free-stream Mach number
M_L	local Mach number
NACA	National Advisory Committee for Aeronautics
NASA	National Aeronautics and Space Administration
PCM	pulse code modulation
PFTF	Propulsion Flight Test Fixture
p_t	local total pressure, psi
$\bar{q}$	local dynamic pressure, psf
RAGE	Rake Airflow Gage Experiment
RBCC	rocket-based combined-cycle
s	standard deviation
α	local angle of attack, deg
α_f	local flank angle of attack, deg

I. Introduction

The F-15B airplane is a two-seat fighter and trainer version of the F-15A high-performance, supersonic air-superiority fighter (both built by McDonnell Douglas Corporation, now The Boeing Company, St. Louis, Missouri) and is powered by twin F100-PW-100 afterburning turbofan engines (Pratt & Whitney, West Palm Beach, Florida). The National Aeronautics and Space Administration (NASA) Dryden (Edwards, California) F-15B airplane has been converted from a United States Air Force air-superiority fighter to a research test bed airplane. Research instrumentation, recording, telemetry, and video systems have been installed in the airplane. A calibrated National Advisory Committee for Aeronautics (NACA)-style flight-test nose boom was installed for measurements of free-stream Mach number, angle of attack, and angle of sideslip. Figure 1 shows the F-15B airplane with the Rake Airflow Gage Experiment (RAGE) during a flight test.

Figure 1. The NASA Dryden F-15B research test bed with Propulsion Flight Test Fixture pylon and Rake Airflow Gage Experiment rake during flight test.

The Propulsion Flight Test Fixture (PFTF), shown in figure 2, mounts to a standard centerline pylon of the NASA Dryden F-15B airplane. It was developed at NASA Dryden for flight-testing propulsion-related experiments such as inlets and nozzles at a range of subsonic and supersonic flight conditions (ref. 1). The PFTF has a length of 107 in., a height of 19 in., and a maximum thickness of 10 in. A significant amount of internal space in the fixture is provided for research instrumentation and propellant storage tanks. Standard PFTF instrumentation includes the following: (1) a six-degree-of-freedom inertial sensing unit, (2) absolute and differential pressure transducers, (3) a total temperature probe, and (4) an integrated six-component force balance capable of measuring forces and moments in all three axes. Research experiments are flown underneath the centerline of the PFTF connected to the force balance hardware. Experimental data obtained during flight tests are sampled and transmitted through the pulse code modulation (PCM) system of the PFTF to the airplane, and can be recorded on board and telemetered down to the ground for real-time monitoring.

Figure 2. Propulsion Flight Test Fixture with Rake Airflow Gage Experiment.

The PFTF has been flown in two previous flight experiments. Using a NACA air data boom mounted to a cylinder and conical nose cap, the Local Mach Investigation (LMI) flights (ref. 2) quantified the local Mach number and flow angle at a single point underneath the F-15B airplane at various flight conditions. Additionally, the Cone Drag Experiment (CDE) flights (ref. 3) tested the drag-measuring capabilities of the PFTF's integrated force balance from subsonic speeds to Mach 2.

To support future propulsion research using this unique flight test fixture, the flow quality underneath the F-15B airplane must be quantified and correlated to the airplane free-stream conditions. The RAGE was designed to measure the Mach number, flow angularity, total pressure distortion, and dynamic pressure in front of the PFTF at the aerodynamic interface plane of the Channeled Centerbody Inlet Experiment (CCIE), an experimental mixed-compression, supersonic inlet (ref. 4) that will be flown on the PFTF in the near future. The data from this experiment are aimed at providing the CCIE and future PFTF experiments with estimates of flow speed, direction, and distortion prior to flight tests.

II. Rake Airflow Gage Experiment

The RAGE involves a flow-field survey rake that was flight-tested on the PFTF using the NASA Dryden F-15B research test bed airplane. This section describes the experiment design and setup in detail.

A. Experiment Design

The RAGE, designed by NASA Dryden, consists of a flow-field survey rake, cylindrical boom, and cone cylinder. Figure 2 shows the RAGE and PFTF mounted to the NASA Dryden F-15B research airplane. The rake, shown in the far right of the picture, is secured to an aluminum boom that is attached to an aluminum cone cylinder. This cone cylinder, known as the crayon because of its shape, is mechanically attached to the PFTF force balance through four bars that bolt to two sleeves on the crayon.

The flow-field survey rake consists of nine five-hole conical probes mounted in a cruciform configuration, as shown in figure 3. The span of the rake is 9.5 in., and the chord is 2.5 in., with a

maximum thickness of 0.375 in. A span of 9.5 in. was chosen to represent the size of a typical experiment on the PFTF. The rake is a two-piece design, comprised of a front and rear section that bolt together. The rake is made of 7075-T6 aluminum, chosen for its high specific strength and ease of machining. A channel between the front and rear sections allows for routing of the probe pressure tubing. This geometry was chosen to accommodate pressure tube routing, bending stress constraints, machining requirements, and wind-tunnel flow blockage concerns.

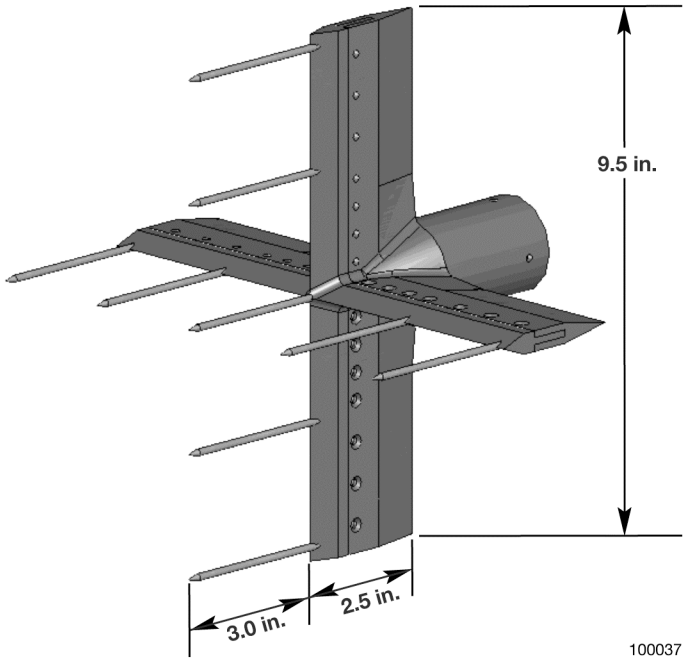

Figure 3. Rake Airflow Gage Experiment flow-field survey rake consisting of nine five-hole conical probes.

The conical probes, manufactured by Aeroprobe Corporation (Blacksburg, Virginia), are fabricated from stainless steel and are comprised of a conical forebody and cylindrical afterbody. Each probe has a diameter of 0.125 in. and a length of 3.75 in. The cap of the probe is a 60-degree right-circular cone with the tip of the cone replaced by a 0.015-in. pitot port situated normal to the longitudinal axis of the cone. Four static pressure ports are located on the surface of the cone. Two ports lie diametrically opposed on the vertical meridian of the cone, and the remaining two are situated in the same fashion on the horizontal meridian. Inconel® alloy 600 (Special Metals Corporation, New Hartford, New York) exit tubulations are connected to the ports for transmission of the cone surface and pitot pressures. Figure 4 shows a schematic of the probe and port numbering convention. The conical probes extend 3.0 inches in front of the leading edge of the rake. This placement helps to ensure that the pressure ports are located forward of any bow shocks originating from the rake body at supersonic conditions.

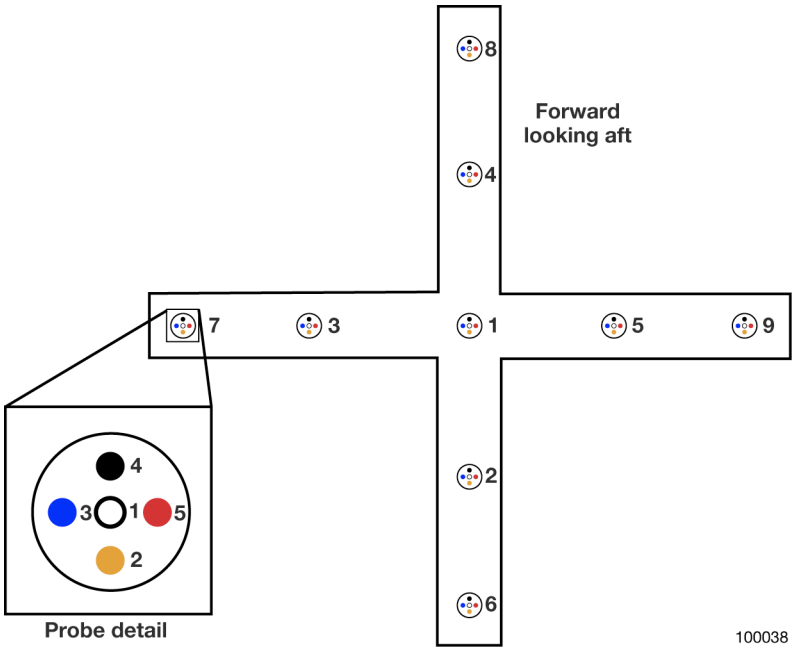

Figure 4. Rake layout and probe and port numbering convention (flight 1).

Before the flight test, the rake was calibrated in the Boeing Polysonic Wind Tunnel in St. Louis, Missouri. Calibration data were taken at various combinations of angles of attack and sideslip out to ± 10° at Mach numbers of 1.46, 1.51, and 1.61. A calibration algorithm for the calculation of local Mach number, flow angularity, total pressure, and dynamic pressure at each of the nine probes was developed and coded for real-time calculations in flight. Table 1 shows the estimated uncertainties in the probe-calculated flow quantities. More detail on the design and calibration of the rake can be found in reference 5.

Table 1. Rake uncertainties.

Quantity	Uncertainty
Mach number	±0.02
α	±0.50°
α_f	±0.50°
p_t	±1%
$\bar{q}$	±1%

B. Experiment Setup

The RAGE flow-field rake was positioned at the aerodynamic interface plane of the Channeled Centerbody Inlet, as depicted in figure 5. The rake was secured in this location by a cylindrical boom that was attached to a cone cylinder. The cone cylinder allows for experiment integration with the PFTF through the force balance assembly. For the RAGE flights, the cone cylinder was inclined towards the underbody of the airplane by 5° measured from a horizontal plane parallel to the waterlines of the airplane. The purpose of inclining the rake was to better align the probes with the local velocity vector during flight at supersonic Mach numbers. Data from the LMI experiment suggest that at supersonic conditions, there is a variable downwash underneath the airplane that ranges from approximately 3 to 8°

over a free-stream Mach range of M_∞= 1.3–2.0. Although the downwash underneath the airplane was expected to exceed 5° at the RAGE test points, the cone cylinder could not be inclined further because of minimum ground clearance requirements when the PFTF is mounted underneath the airplane.

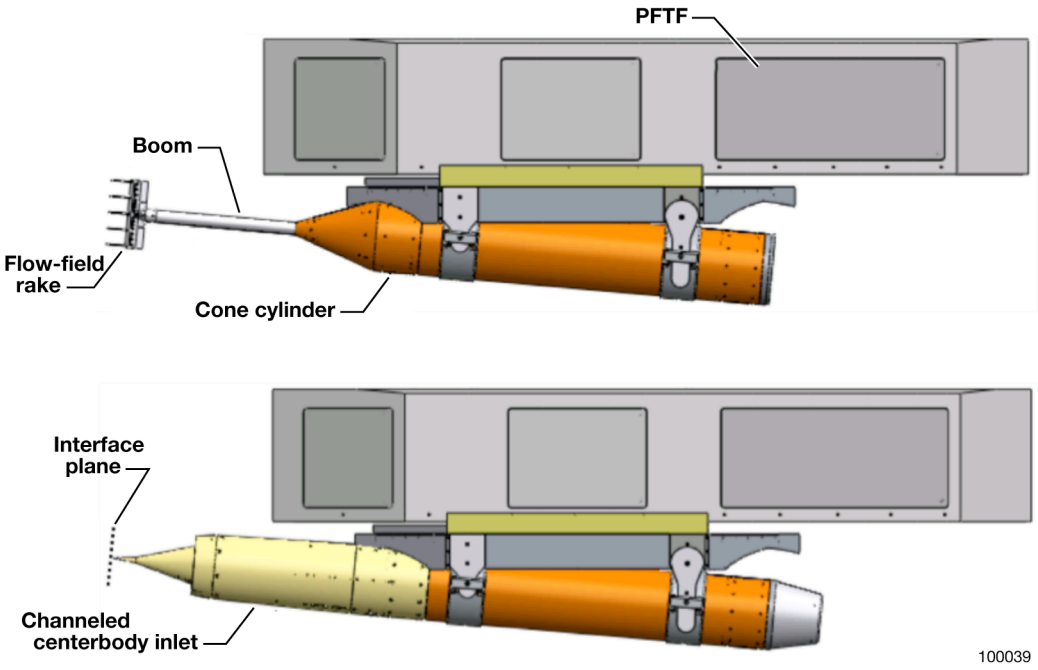

Figure 5. Comparison of Rake Airflow Gage Experiment configuration with Channeled Centerbody Inlet Experiment configuration, showing the aerodynamic interface plane.

Flexible urethane tubing was drawn through the cone cylinder and boom hardware to connect the probe tubulations, which terminated at the back of the rake, to differential pressure scanners mounted on the instrumentation tray located underneath the PFTF force balance. A single ±30-psid 32-port electronically scanned differential pressure transducer was used to measure the pitot pressures of each of the nine conical probes, while two ±15-psid 32-port electronically scanned differential pressure transducers were used to measure the surface static pressures on the RAGE probes. A known reference pressure was plumbed to the reference ports on the three differential pressure transducers. The reference pressure selected for these three transducers was provided by four cone surface static measurements taken from a separate conical probe that is located on the front of the PFTF. The four static ports of the PFTF probe were connected to a manifold inside the PFTF. The output from the manifold was connected to the reference pressure ports on each differential pressure transducer and to a 15-psia absolute pressure transducer for an accurate measurement of the reference pressure. Before the flight, the pressure tubing from the conical probes to the differential pressure transducers was checked extensively to identify and correct any excessive leaks in the system. All 45 pressure ports had leak rates that were within the noise level of the differential pressure transducers (0.05 psi) and were deemed acceptable for the purposes of this experiment.

III. Flight Test

The experimental data for the RAGE program were obtained during two separate research flights that were conducted in the second half of 2009. This section describes the objectives, approach, and results from the flight test in detail.

A. Objectives and Approach

The primary objective of the RAGE was to quantify the local flow field (Mach number, flow angularity, total pressure distortion, and dynamic pressure) at the aerodynamic interface plane of the CCIE and to correlate this flow field to airplane free-stream conditions. The CCIE was designed and sized to provide a specific mass flow to a notional rocket-based combined-cycle (RBCC) (ref. 6) engine at a local Mach number, M_L, of 1.5 with a local dynamic pressure, $\bar{q}$, of 1,000 psf. As a result, the identification of the free-stream Mach number that results in $M_L = 1.5$ at the inlet interface plane, along with measurements of the local flow angularity, total pressure distortion, and dynamic pressure at $M_L = 1.5$, were of primary importance to the RAGE. Of secondary importance was the determination of $M_L = 1.6$, because this test point is a possible test point for the CCIE. This particular Mach number also represents the upper end of the rake's calibration. Using nine probes in a cruciform array, as opposed to a single probe, allows for the determination of a more robust average interface plane value for each flow property and also provides information on flow uniformity over the interface plane. Because the CCIE is not an axisymmetric inlet, the identification of nonuniformities in the local flow field is important to assist with test point planning and the interpretation of the flight test results for that program. The flow-field data obtained from the RAGE will be used primarily for flight-test planning and computational flow analysis of the CCIE, but they are applicable to any other propulsion-related experiment that might fly on the PFTF in the future.

A total of two flights were conducted for the RAGE. The first flight, occurring in August of 2009, was the primary research flight for this program in which the bulk of the data was obtained. Therefore, the data from this flight are discussed in greater detail. A second flight was conducted in October of 2009 to spot-check some anomalous data that had been observed at a particular location on the interface plane during the first flight. For this flight, the rake was rotated 180° about its longitudinal axis to ensure that the data anomaly was not the result of a particular probe.

For both flights, experimental data were obtained at steady-state supersonic test points and during the straight and level acceleration segments out to these points. Because the relationship between free-stream and local conditions was not known before the first flight, the desired steady-state test points had to be identified in real time during the flight by using the calculated local flow properties, available in the control room, to guide the pilot to the target free-stream Mach number that produced the desired local Mach number. Flow-field data were obtained primarily at a pressure altitude of 40,000 ft, because this altitude allowed for test points to be flown up to $M_\infty = 2$, if necessary, to achieve the desired local flow conditions. For the first run on the first flight, a steady-state test point at $M_\infty = 1.65$ was chosen to develop an initial correlation between the free-stream and local flow quantities. The data from this first run identified $M_\infty = 1.56$ as a desired test point for the second run. On the second run, the airplane accelerated out to $M_\infty = 1.56$, held this condition for 10 s, then accelerated out to $M_\infty = 1.86$, at which point the pilot was instructed to hold the condition for another 10 s, because the upper Mach limit of the rake's calibration had been reached. For the first flight, a total of four supersonic runs, with aerial refueling in between each run, were necessary to obtain test data at a range of supersonic Mach numbers. During this flight, test points were also flown at pressure altitudes of 35,000 and 45,000 ft to check for altitude effects on the local flow properties. Figure 6 shows a summary of the flight conditions in which data were obtained. A total of seven unique steady-state test points over a range of free-stream Mach numbers from 1.56 to 1.86 were flown. To check for data repeatability, the $M_\infty = 1.56$ and 1.86 test points at 40,000 ft were repeated on run 3 of the first flight. For the second flight, the $M_\infty = 1.56$, 1.65, and 1.86 test points at 40,000 ft were flown for comparison with the data obtained at these conditions on the first flight. Table 2 shows the aggregate of steady-state test points for both flights.

Table 2. Steady-state test points.

Pressure altitude, ft	Mach number	Run	Flight
40,000	1.65	1	1
40,000	1.56	2	1
40,000	1.86	2	1
40,000	1.56	3	1
40,000	1.86	3	1
35,000	1.75	3	1
45,000	1.56	4	1
45,000	1.86	4	1
35,000	1.56	4	1
40,000	1.56	1	2
40,000	1.65	1	2
40,000	1.86	1	2

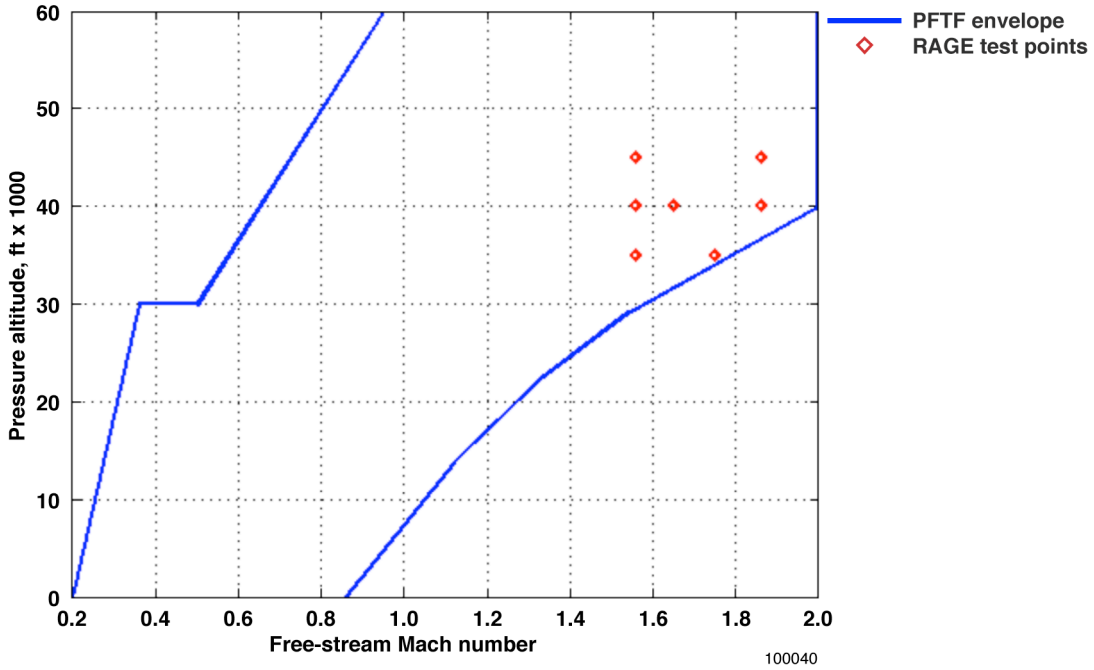

Figure 6. Rake Airflow Gage Experiment steady-state test points.

B. Flight Test Results

Note that probes 1, 6, and 7 were unintentionally bent by small amounts during the aforementioned leak checks of the pressure tubing. The probes were straightened as much as possible; however, reorienting them in the exact same configuration as they had been during the wind-tunnel calibration of the rake was impossible. Consequently, the flow calculations from these three probes have an additional error associated with them. Although the data obtained from these three probes are presented, they are not discussed in detail in this report. Also note that the local angle of attack that is discussed in this report is measured with respect to the inclined rake. Therefore, it is necessary to subtract 5° to these values to

obtain the total angle of attack underneath the airplane with respect to the longitudinal axis of the airplane.

To facilitate presentation of the steady-state data, the calculated flow properties for each probe were time averaged over the test point duration. The time-averaged flow properties from the six unbent probes (2, 3, 4, 5, 8, and 9) were used to compute the mean flow conditions over the interface plane. In addition to the steady-state flow properties, the level acceleration flow-field calculations also are presented. Because the pressure transducers are located several feet away from the pressure ports of the probes, the pressures measured during the acceleration portion of the run are different from the true pressures because of the lag caused by the tubing. Based on the methods given in Gracey (ref. 7) and Huston (ref. 8), the pressure lag of the system during the acceleration was estimated to have a mean value of approximately 0.005 psi. Because this value was within the measurement resolution of the differential pressure transducers, the pressure lag of the tubing was deemed negligible. It should be noted, however, that the calculation method is only rigorously valid for straight lengths of tubing. As a result, the acceleration data should be considered an approximation of the behavior of the local flow properties during those maneuvers.

C. Local Mach Number, Total Pressure Distortion, and Dynamic Pressure

The local Mach number measured during the RAGE flights was expected to be less than the free-stream value as a result of the airplane flying faster than the speed of sound. At supersonic speeds, the airplane surfaces, particularly the nose and inlet ramps, produce oblique shock waves that alter the flow underneath the airplane. As the free-stream flow passes through these shock waves, it undergoes a reduction in Mach number and is turned away from the airplane underbody. In addition to the airplane-generated shock waves, several other factors, including but not limited to, variable inlet spillage, dissimilar trim settings between port and starboard engines, and airplane attitude are thought to affect the local flow conditions underneath the airplane.

1. Steady-State Results

Tables 3–7 present the time-averaged steady-state data for both flights. The local Mach number, total pressure, and dynamic pressure for the unbent probes were used to calculate the mean and standard deviation of these quantities over the interface plane. For the first flight, the 40,000-ft test points, shown in table 3, indicate that the average local Mach number at the inlet interface plane varies from 1.48 to 1.60 over a free-stream Mach range of 1.56–1.86. The data in table 3 indicate that a free-stream Mach number of 1.65 will achieve the desired local Mach number of 1.5 for the CCIE. Small deviations from the mean Mach number of up to 0.03 are apparent from a probe-to-probe comparison. The variances in local Mach number between the probes show that the flow at the interface plane is not entirely uniform. As a check of the data repeatability, the $M_\infty = 1.56$ and 1.86 test points at 40,000 ft were repeated on the third run of flight 1. The average local Mach number from the repeated test points showed excellent agreement between the two runs, as seen in table 4.

Table 3. Rake Airflow Gage Experiment flow-field summary (flight 1, 40,000 ft).

$M_\infty = 1.56$					
Probe	M_L	α, deg	α_f, deg	p_t, psi	$\bar{q}$, psf
1*	1.49	–0.60	0.22	10.96	678
2	1.48	–0.81	–0.11	10.97	679
3	1.48	–0.01	–0.68	10.94	677
4	1.49	–1.30	0.25	10.95	677
5	1.50	–1.40	–0.19	10.99	679
6*	1.47	0.67	1.85	11.03	683
7*	1.49	–1.12	–0.77	10.95	677
8	1.48	–1.15	0.15	10.84	671
9	1.46	–0.53	0.87	10.89	675
m	1.48	–0.87	0.05	10.93	676
s	0.01	0.53	0.52	0.06	3
			Distortion	1.4%	
$M_\infty = 1.65$					
Probe	M_L	α, deg	α_f, deg	p_t, psi	$\bar{q}$, psf
1*	1.51	–1.63	1.05	12.33	761
2	1.50	–2.73	0.12	12.41	767
3	1.52	–0.83	–0.35	12.37	763
4	1.52	–1.75	0.16	12.27	757
5	1.52	–2.06	–0.22	12.39	764
6*	1.49	–1.36	1.78	12.50	773
7*	1.51	–2.41	–0.30	12.37	763
8	1.51	–2.07	0.01	12.20	753
9	1.47	–1.05	0.20	12.24	758
m	1.50	–1.75	–0.01	12.31	760
s	0.02	0.71	0.22	0.09	5
			Distortion	1.7%	
$M_\infty = 1.86$					
Probe	M_L	α, deg	α_f, deg	p_t, psi	$\bar{q}$, psf
1*	1.62	–3.34	1.30	16.43	993
2	1.62	–4.82	0.27	16.68	1009
3	1.62	–3.26	0.07	16.46	995
4	1.59	–3.31	–0.28	16.10	979
5	1.61	–4.19	0.18	16.46	998
6*	1.60	–2.82	1.28	16.79	1019
7*	1.63	–4.37	0.28	16.67	1004
8	1.58	–3.92	0.22	15.75	961
9	1.58	–3.19	–0.06	16.38	998
m	1.60	–3.78	0.07	16.30	990
s	0.02	0.65	0.20	0.33	17
			Distortion	5.7%	
* Denotes bent probe					

Table 4. Rake Airflow Gage Experiment flow-field summary (flight 1, 40,000 ft, repeated test points).

$M_\infty = 1.56$					
Probe	M_L	α, deg	α_f, deg	p_t, psi	$\bar{q}$, psf
1*	1.48	–0.65	0.29	10.93	677
2	1.48	–0.96	–0.11	10.96	678
3	1.48	0.05	–0.66	10.93	676
4	1.49	–1.18	0.25	10.95	677
5	1.50	–1.38	–0.04	10.97	678
6*	1.47	0.71	2.01	11.01	682
7*	1.49	–1.05	–0.82	10.94	677
8	1.48	–1.06	0.17	10.82	670
9	1.46	–0.49	0.93	10.89	675
m	1.48	–0.84	0.09	10.92	676
s	0.01	0.53	0.52	0.06	3
			Distortion	1.4%	
$M_\infty = 1.86$					
Probe	M_L	α, deg	α_f, deg	p_t, psi	$\bar{q}$, psf
1*	1.61	–3.26	1.26	16.08	974
2	1.61	–4.73	0.30	16.30	987
3	1.61	–3.12	0.09	16.10	975
4	1.58	–3.32	–0.33	15.76	962
5	1.60	–4.10	0.14	16.13	979
6*	1.60	–2.67	1.33	16.51	1002
7*	1.62	–4.33	0.28	16.26	982
8	1.57	–3.88	0.25	15.44	944
9	1.58	–3.12	–0.16	16.15	985
m	1.59	–3.71	0.05	15.98	972
s	0.02	0.64	0.24	0.32	17
			Distortion	5.4%	
* Denotes bent probe					

Table 5. Rake Airflow Gage Experiment flow-field summary (flight 1, 45,000 ft).

$M_\infty = 1.56$					
Probe	M_L	α, deg	α_f, deg	p_t, psi	$\bar{q}$, psf
1*	1.51	–0.67	0.81	8.73	539
2	1.49	–0.51	0.37	8.72	539
3	1.49	–0.27	–0.41	8.69	538
4	1.51	–0.99	0.09	8.73	538
5	1.51	–1.19	0.39	8.73	539
6*	1.48	0.55	1.85	8.77	543
7*	1.50	–1.22	–0.40	8.70	538
8	1.49	–0.89	0.54	8.60	532
9	1.47	–0.20	1.06	8.66	537
m	1.49	–0.67	0.34	8.69	537
s	0.01	0.41	0.49	0.05	3
			Distortion	1.5%	
$M_\infty = 1.86$					
Probe	M_L	α, deg	α_f, deg	p_t, psi	$\bar{q}$, psf
1*	1.61	–3.07	1.60	12.37	747
2	1.60	–4.17	0.28	12.50	756
3	1.60	–2.71	0.28	12.38	748
4	1.58	–3.29	0.00	12.12	736
5	1.60	–3.60	0.28	12.36	747
6*	1.57	–2.30	1.48	12.20	743
7*	1.61	–3.59	0.42	12.60	759
8	1.56	–3.90	0.42	11.86	723
9	1.56	–2.76	0.41	12.23	746
m	1.58	–3.41	0.28	12.24	743
s	0.020	0.597	0.152	0.229	11
			Distortion	5.2%	
* Denotes bent probe					

Table 6. Rake Airflow Gage Experiment flow-field summary (flight 1, 35,000 ft).

$M_\infty = 1.56$					
Probe	M_L	α, deg	α_f, deg	p_t, psi	$\bar{q}$, psf
1*	1.48	–0.76	0.31	13.64	845
2	1.47	–1.16	–0.06	13.67	847
3	1.48	–0.11	–0.43	13.67	846
4	1.48	–1.09	0.64	13.61	843
5	1.48	–1.46	0.06	13.68	847
6*	1.47	0.16	1.84	13.79	854
7*	1.48	–1.61	–0.19	13.68	847
8	1.48	–1.35	0.05	13.52	837
9	1.46	–0.48	0.10	13.61	844
m	1.47	–0.94	0.06	13.63	844
s	0.01	0.53	0.34	0.06	4
			Distortion	1.2%	
$M_\infty = 1.75$					
Probe	M_L	α, deg	α_f, deg	p_t, psi	$\bar{q}$, psf
1*	1.53	–2.93	1.20	17.34	1067
2	1.54	–3.15	0.07	17.48	1073
3	1.53	–3.01	0.00	17.33	1067
4	1.52	–2.07	0.35	17.15	1057
5	1.54	–3.27	0.13	17.50	1074
6*	1.56	–1.42	1.63	17.71	1083
7*	1.56	–3.29	0.52	17.42	1067
8	1.53	–3.06	0.42	17.03	1048
9	1.53	–2.33	0.13	17.54	1080
m	1.53	–2.81	0.18	17.34	1066
s	0.01	0.49	0.17	0.21	12
			Distortion	2.9%	
* Denotes bent probe					

Table 7. Rake Airflow Gage Experiment flow-field summary (flight 2, 40,000 ft).

$M_\infty = 1.56$					
Probe	M_L	α, deg	α_f, deg	p_t, psi	$\bar{q}$, psf
1*	1.49	–0.94	0.11	10.82	669
2	1.49	–1.20	–0.50	10.74	665
3	1.49	–1.42	0.56	10.82	669
4	1.49	–1.43	0.01	10.87	672
5	1.49	–0.71	–0.83	10.78	667
6*	1.48	–2.03	–1.26	10.65	660
7*	1.49	–0.37	1.41	10.81	669
8	1.46	–0.80	0.05	10.83	671
9	1.48	–0.57	–1.68	10.78	668
m	1.48	–1.02	–0.40	10.80	669
s	0.01	0.38	0.79	0.04	3
			Distortion	1.1%	
$M_\infty = 1.65$					
Probe	M_L	α, deg	α_f, deg	p_t, psi	$\bar{q}$, psf
1*	1.51	–2.40	–0.55	12.11	747
2	1.50	–1.99	–0.27	11.93	737
3	1.52	–2.42	1.18	12.15	749
4	1.49	–3.42	0.28	12.13	750
5	1.50	–1.42	–1.00	12.04	744
6*	1.50	–2.45	–1.23	11.87	733
7*	1.50	–1.84	0.68	12.10	748
8	1.47	–2.16	0.26	12.13	752
9	1.50	–1.60	–1.45	12.07	746
m	1.50	–2.17	–0.17	12.08	746
s	0.02	0.71	0.95	0.08	5
			Distortion	1.9%	
$M_\infty = 1.86$					
Probe	M_L	α, deg	α_f, deg	p_t, psi	$\bar{q}$, psf
1*	1.64	–4.46	–0.18	16.27	979
2	1.60	–3.43	0.41	15.75	957
3	1.59	–4.99	–0.17	16.03	975
4	1.61	–4.46	0.14	16.33	989
5	1.62	–3.43	–0.70	16.18	977
6*	1.57	–4.33	–1.44	15.37	939
7*	1.61	–3.65	0.43	16.22	983
8	1.59	–3.66	0.02	16.43	1001
9	1.62	–3.81	–0.38	16.35	988
m	1.60	–3.96	–0.11	16.18	981
s	0.02	0.63	0.39	0.25	15
			Distortion	4.2%	
* Denotes bent probe					

Between M_∞ = 1.56 and 1.86, the mean local total pressure, p_t, at the interface plane ranged from approximately 10.9 to 16.3 psi, with small deviations apparent between the individual probes. The total pressure deviations are representative of distortion in the local flow field. Equation (1) was used as a simple measure of the local distortion, and the distortion was calculated to have a range of 1.4–5.7 percent over M_L = 1.48–1.60. At M_L = 1.5, the distortion is less than 2 percent, which is an acceptable value for the CCIE. Interestingly, there appears to be a total pressure deficit of 0.55 psi at the top of the rake (probe 8) during the M_∞ = 1.86 test point. This total pressure deficit is the primary reason for the elevated level of distortion at this Mach number.

$$\text{Distortion } \% = \left(\frac{p_{t,\max} - p_{t,\min}}{p_{t,avg}} \right) \times 100 \tag{1}$$

The local dynamic pressure at the 40,000-ft steady-state test points ranged from approximately 680 to 990 psf. These values are well within the PFTF limit of 1,100 psf, suggesting that higher local Mach test points could be achieved at 40,000 ft, if necessary, for the CCIE or other potential future experiments. As previously mentioned, the target dynamic pressure for the CCIE at its design speed of M_L = 1.5 is 1,000 psf. This value was determined to be required to provide a specific mass flow to a conceptual RBCC engine that is no longer in development. At M_L = 1.5, the measured dynamic pressure is approximately 760 psf. Because dynamic pressure has a second-order effect on the performance of the inlet, the repercussions of flying the M_L = 1.5 test point at this lower dynamic pressure should be negligible. Alternatively, it would be possible to fly the CCIE at a greater local dynamic pressure by flying at the same local Mach number, but at a lower pressure altitude.

During the first flight, additional test points were flown at 45,000 and 35,000 ft to check for altitude effects on the local flow conditions at the interface plane. Tables 5 and 6 show the results from the steady-state test points for the pressure altitude runs at 45,000 and 35,000 ft, respectively. The data obtained at these altitudes show that the local Mach number and distortion for a given free-stream Mach number are effectively the same among the three altitudes flown during the flight test. In contrast to local Mach number and distortion, the local dynamic pressure between the different pressure altitudes will not be the same, as it is dependent on the free-stream pressure, and thus the pressure altitude. Because of the dynamic pressure limits on the PFTF, the maximum free-stream Mach number at 35,000 ft was limited to 1.75. As shown in table 5, the average local Mach number at this condition was 1.53. The total pressure distortion was 2.9 percent with a mean dynamic pressure of 1,066 psf. This particular test point represents the highest local Mach number that experiments can be flown using the PFTF at 35,000 ft.

The second flight consisted of one supersonic run with steady-state test points at M_∞ = 1.56, 1.65, and 1.86 at 40,000 ft. Table 7 presents the results from this flight. A comparison of tables 3 and 7 shows that the average local Mach numbers were in excellent agreement with those measured during the first flight. The total pressure distortion at the two lower Mach test points were in good agreement. At M_∞ = 1.86, the total pressure distortion was calculated to be 4.5 percent, some 1.2 percent lower than that obtained from the first flight. A likely reason for this sizeable difference is that the rake was inverted for the second flight. Inverting the rake placed probe 6 at the top location on the rake, a region where the largest total pressure deficit was seen during the first flight. Since probe 6 was one of the bent probes, the data were not included in the distortion calculation. In table 8, the mean interface plane flow quantities from both flights were averaged to produce a final correlation between airplane free-stream Mach number and the local flow conditions at the aerodynamic interface plane at 40,000 ft. The correlation from this table should prove useful in the flight test planning of the CCIE and future PFTF projects.

Table 8. Average interface plane quantity from flights 1 and 2.

	40,000 ft		
	M_∞= 1.56	M_∞ = 1.65	M_∞ = 1.86
M_L	1.48	1.50	1.60
α, deg	–0.94	–1.96	–3.87
α_f, deg	–0.17	–0.09	–0.02
p_t, psi	10.87	12.19	16.24
$\bar{q}$, psf	672	753	986

2. Level Acceleration Results

As discussed previously, the pressure lag during the acceleration portion of the supersonic runs was estimated at approximately 0.005 psi. This value was less than the noise level of the pressure transducers, making it reasonable to examine the acceleration data without correcting the measured pressures for lag. Figure 7 shows a comparison between flights 1 and 2 of the mean interface plane Mach number (fig. 7a) and local dynamic pressure (fig. 7b) as a function of airplane free-stream Mach number. The local Mach number and dynamic pressure generally show good agreement between the two flights. The relationship between local and free-stream Mach number is fairly linear with a change in slope at approximately M_∞ = 1.74. Another item of interest from figure 7a is the sharp drop off of approximately 0.02 in the local Mach number as the engine power is reduced for the M_∞ = 1.86 steady-state test point. An examination of the pressure data from the probes showed what appeared to be significant pressure rises of varying magnitude on all of the probes as the engine power setting was reduced to hold the condition at the steady-state test point. After the engine trimmed at the reduced power setting, the probe pressures fell to levels lower than they had previously attained before the reduction in the power setting. This reduction in pressure resulted in a decrease of approximately 0.02 in the local Mach number as seen on the plot. This behavior was observed to a smaller extent at the M_∞ = 1.65 test point yet was absent at the M_∞ = 1.56 test point.

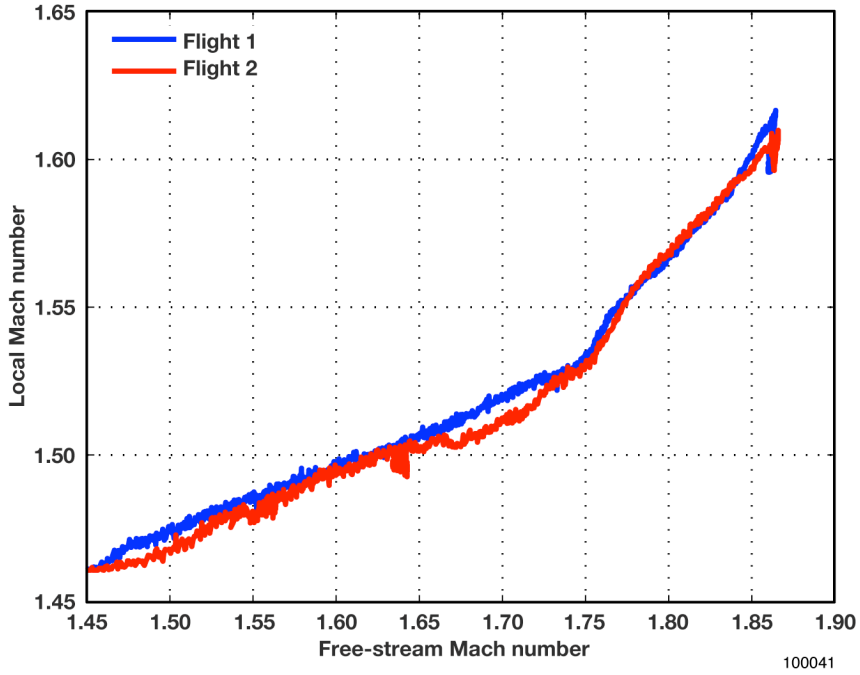

Figure 7a. Mach number.

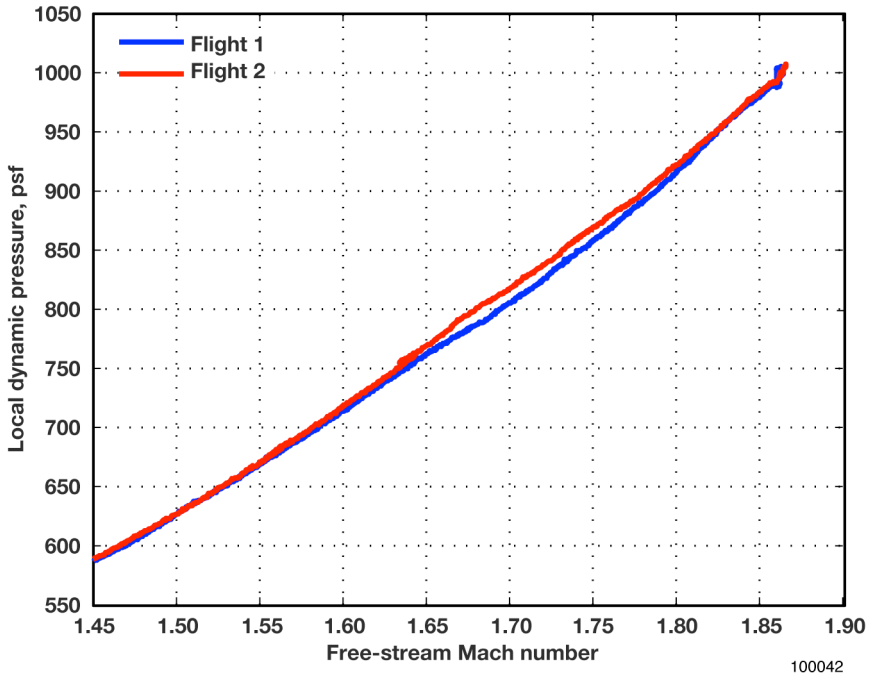

Figure 7b. Dynamic pressure.

Figure 7. Average local Mach number and dynamic pressure during the 40,000-ft supersonic acceleration runs.

D. Local Flow Angularity

The airplane surfaces, particularly the nose and variable position inlet ramps, generate oblique shock waves when the airplane is traveling faster than the speed of sound. These shock waves turn the flow and alter the local flow angularity underneath the airplane. Inlet spillage, which is a function of free-stream Mach number, also is thought to affect the flow angularity underneath the airplane. This section provides a detailed description of the results of the local flow angularity measurements.

1. Steady-State Results

Tables 3–7 provide the time-averaged local flow angularity measurements for the steady-state test points. As discussed previously, the local angle of attack was measured with respect to the experiment, which was inclined 5° above a horizontal plane parallel to the waterlines of the airplane. In general, the data showed the presence of a negative angle of attack or downwash on the rake at all flight conditions in which the rake was within its Mach number calibration range. This downwash is a result of the free-stream flow being turned away from the underbody of the airplane as it passes through the oblique shock waves generated by the airplane. As the free-stream Mach number changes, the angles of the oblique shocks change, which results in the local angle of attack being a function of the free-stream Mach number. Moreover, the inlet ramps are scheduled to provide the appropriate mass flow to the engines over a wide range of Mach numbers. Inlet ramp deflection and spillage, which are functions of free-stream Mach number, also help create the variable flow angularity underneath the airplane.

Table 3 shows the flow angularity results from flight 1 at a pressure altitude of 40,000 ft. During the supersonic run, the downwash underneath the airplane increased with free-stream Mach number. From a free-stream Mach number of 1.56 to 1.86, the average local angle of attack at the interface plane varied from –0.87° to –3.8°, while the average local flank angle was essentially 0°. At the CCIE design Mach number of $M_L = 1.5$, the local downwash is approximately –1.75°. Although not optimal, this level of downwash is still an acceptable level for the CCIE. Tables 5 and 6 show the time-averaged flow angularity for the pressure altitude points at 45,000 and 35,000 ft, respectively. Overall, the data obtained at the $M_\infty = 1.56$ and 1.86 test points showed no significant differences from those obtained at the same free-stream Mach numbers at 40,000 ft. The 35,000-ft, $M_\infty = 1.75$ test point resulted in a mean local angle of attack and flank angle of 2.8° and 0.2°, respectively.

Table 7 provides the flow angularity data from flight 2. Compared with flight 1, for a given free-stream Mach number, the mean local angle of attack measured during flight 2 was more negative; that is, the downwash was greater. The biggest discrepancy between the two flights was at the $M_\infty = 1.65$ test point, in which the mean local downwash on the second flight was approximately 0.4° greater than that measured during the first flight. Potential sources of these discrepancies are discussed in section III-D-3, “Sources of Flow Angularity Discrepancies Observed Between Flights.”

To better understand the flow behavior from over the interface plane, contour plots of both angle of attack and flank angle were generated. Figures 8–11 show the flow angularity contours for flight 1. In the plots, the unbent RAGE probes are shown as black circles, and the bent probes are represented by red circles. The inlet cowl of the follow on experiment, the CCIE, is shown as a dashed black line. It was necessary to include the data from the bent probes in the generation of these plots because of the algorithm that was used to extrapolate the probe data over the entire inlet area. The flow angularity in the region of the bent probes should be viewed with caution for the reasons discussed previously. The figures show that both the angle of attack and flank angle are not uniform across the interface plane, and that the flow angularity is mostly downwash that increases with Mach number. Interestingly, these figures show a reduced region of downwash at probe 3, located directly starboard to the center probe. This downwash deficit, compared to the other probes, was the reason for conducting the second flight with the rake inverted, thereby placing a different probe in that same area of interest. For comparison with the first

flight, figures 12–14 show the flow angularity contours from the second flight. Although the absolute values of flow angularity were different between flights 1 and 2, the angularity trends were similar, particularly when the downwash was considered. The downwash deficit that was seen on the first flight was still present at the location starboard of the center probe. The variable flow angularity over the interface plane, particularly at the location starboard to the center probe, is not optimal, but it is not thought to be excessively detrimental to the future flight test of the CCIE.

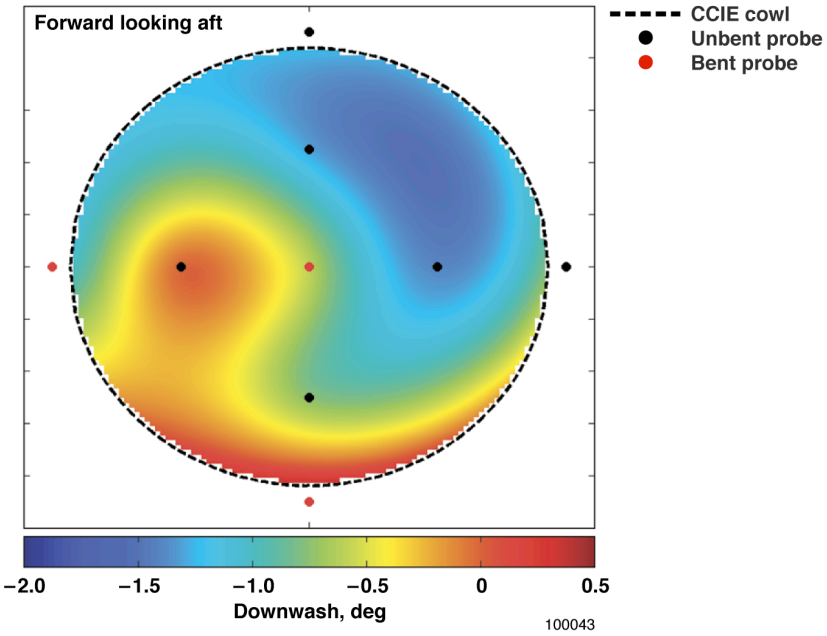

Figure 8a. Angle of attack.

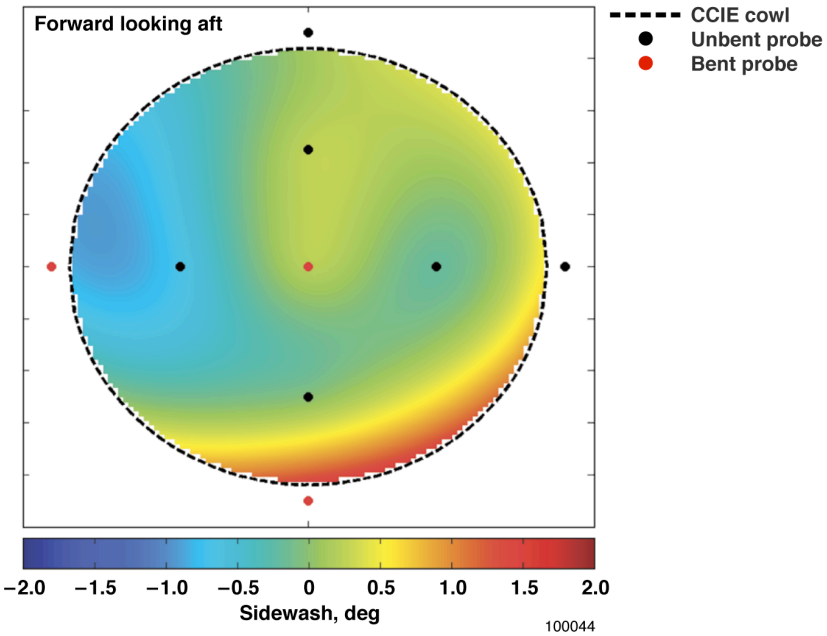

Figure 8b. Flank angle of attack.

Figure 8. Flow angularity contours at a free stream Mach number of 1.56 at 40,000 ft (flight 1).

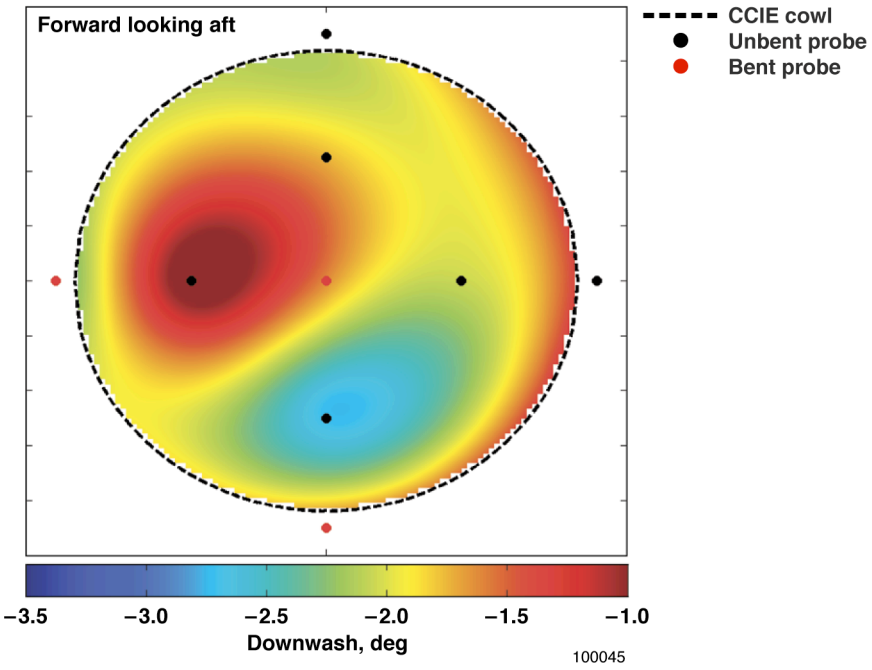

Figure 9a. Angle of attack.

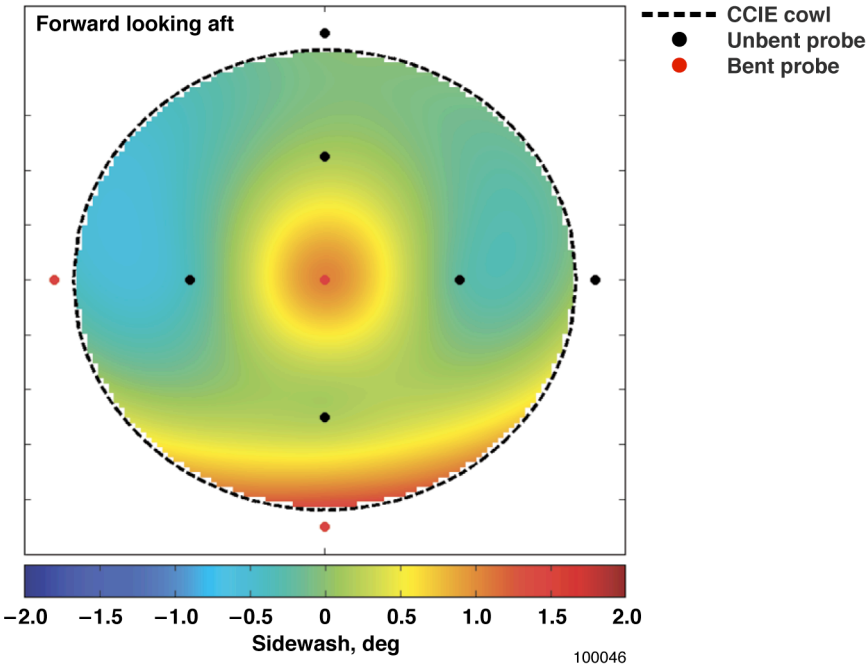

Figure 9b. Flank angle of attack.

Figure 9. Flow angularity contours at a free stream Mach number of 1.65 at 40,000 ft (flight 1).

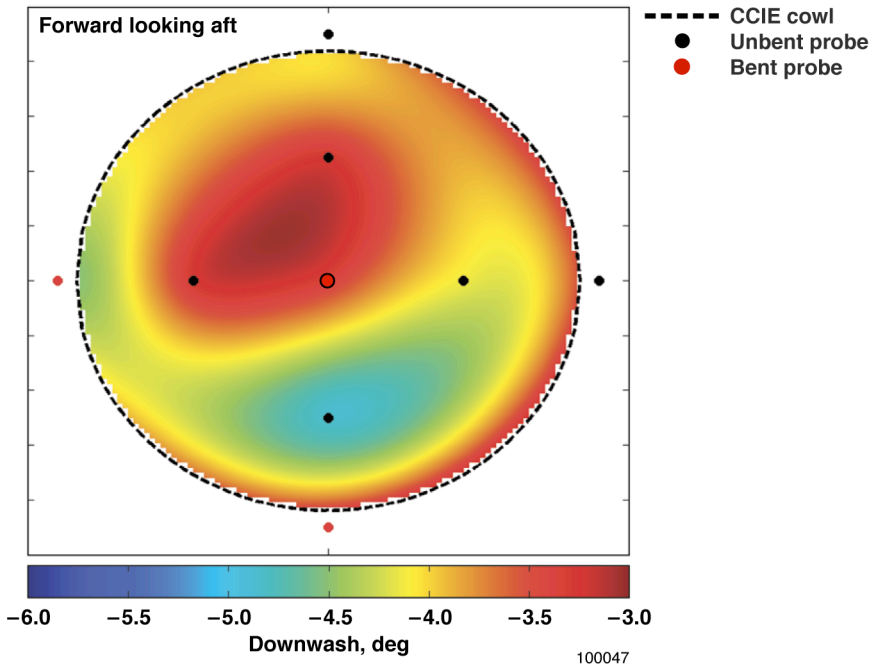

Figure 10a. Angle of attack.

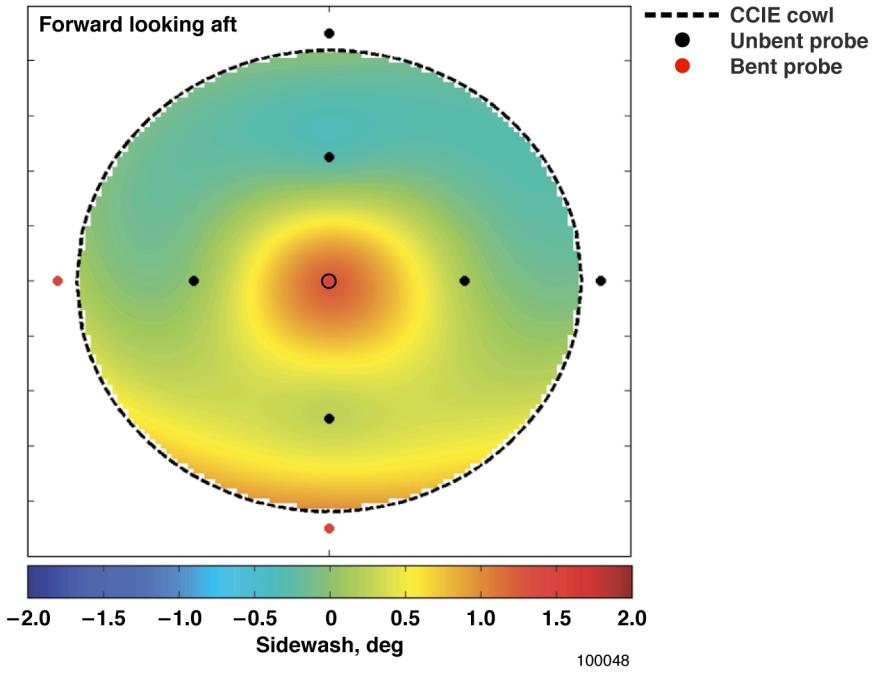

Figure 10b. Flank angle of attack.

Figure 10. Flow angularity contours at a free stream Mach number of 1.86 at 40,000 ft (flight 1).

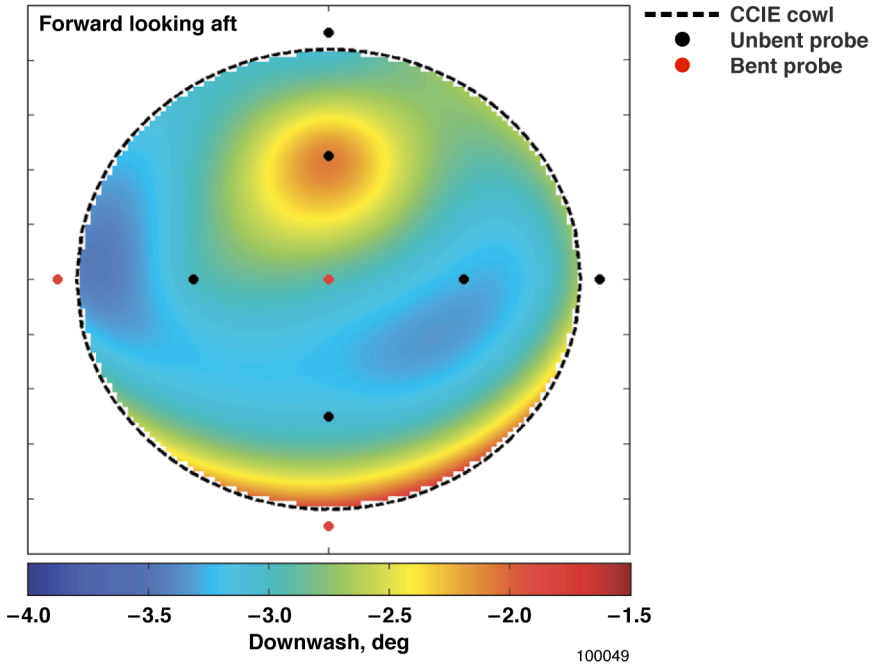

Figure 11a. Angle of attack.

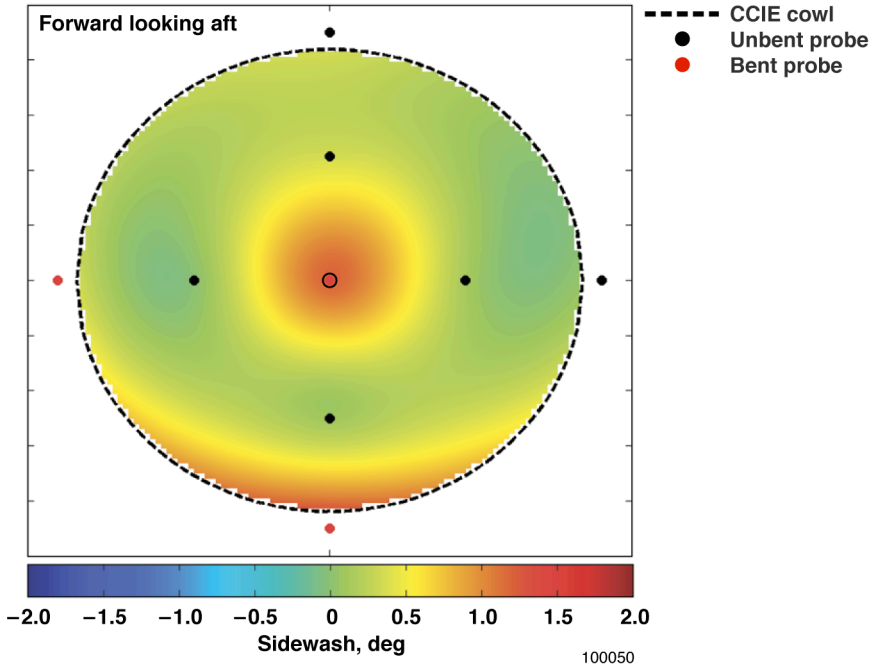

Figure 11b. Flank angle of attack.

Figure 11. Flow angularity contours at a free stream Mach number of 1.75 at 35,000 ft (flight 1).

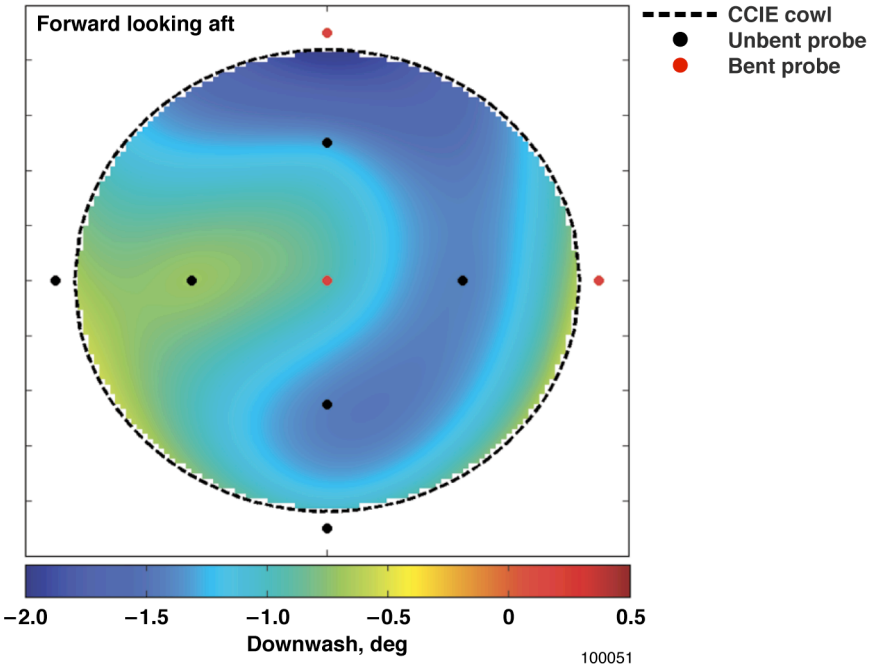

Figure 12a. Angle of attack.

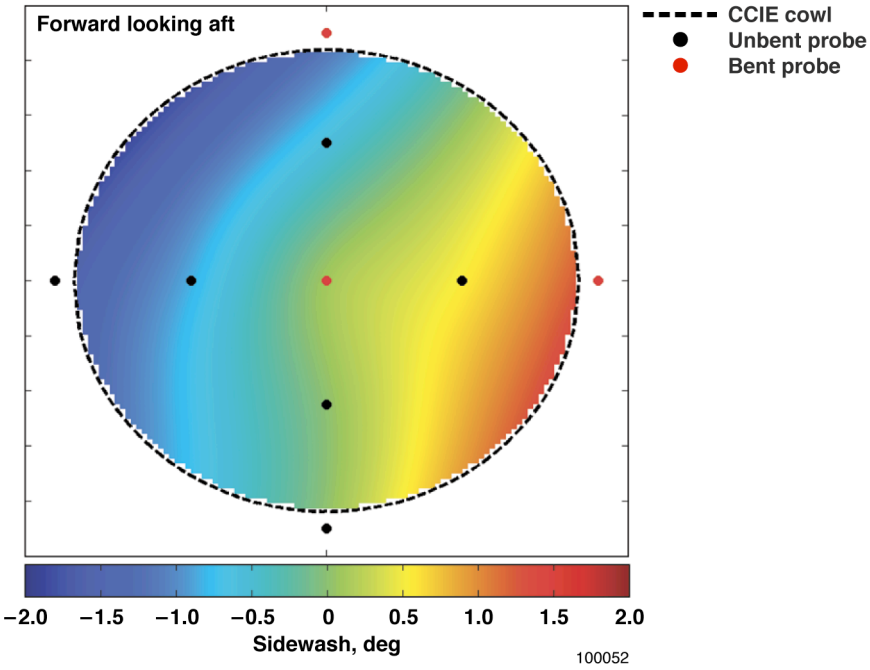

Figure 12b. Flank angle of attack

Figure 12. Flow angularity contours at a free stream Mach number of 1.56 at 40,000 ft (flight 2).

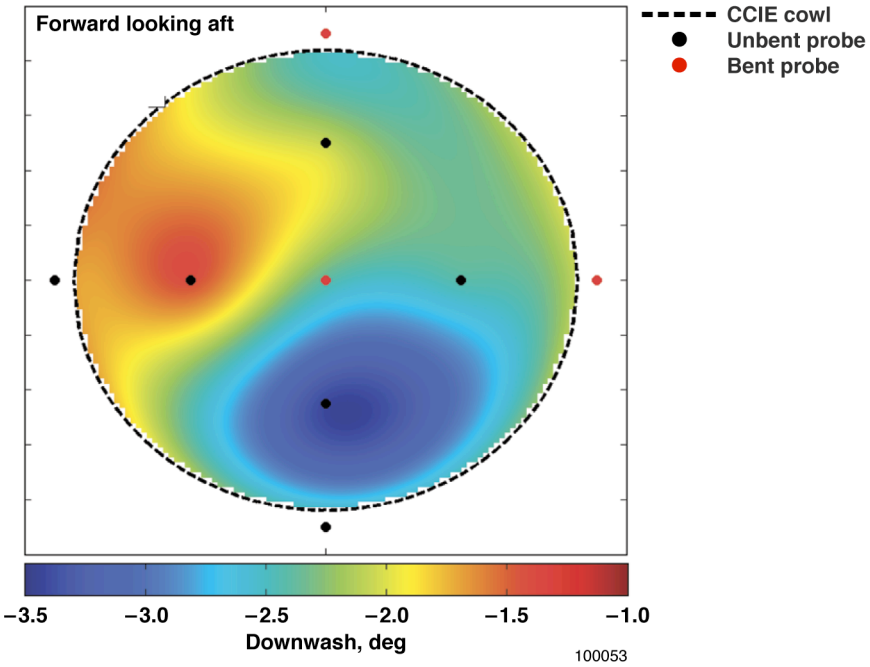

Flight 13a. Angle of attack.

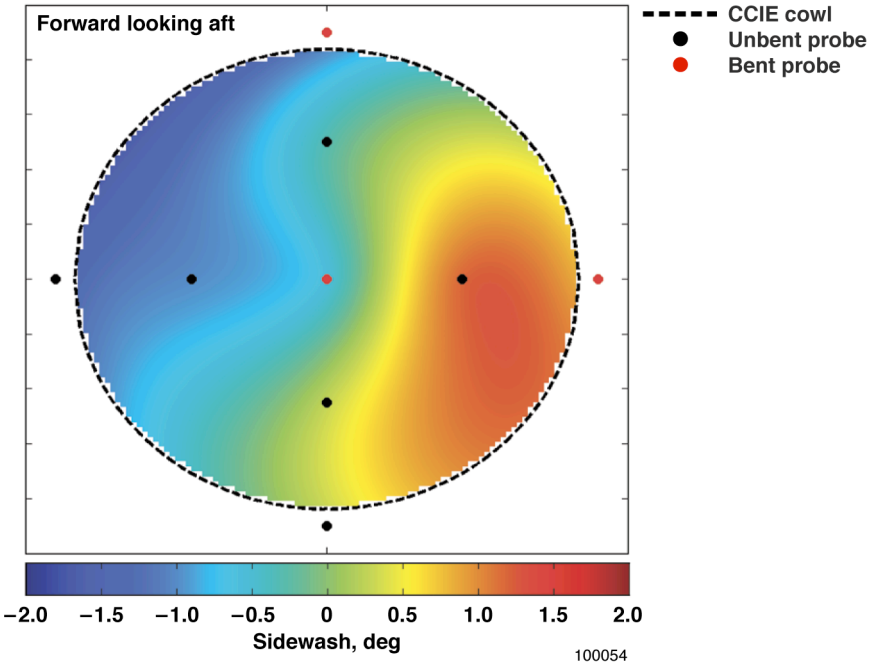

Flight 13b. Flank angle of attack.

Figure 13. Flow angularity contours at a free stream Mach number of 1.65 at 40,000 ft (flight 2).

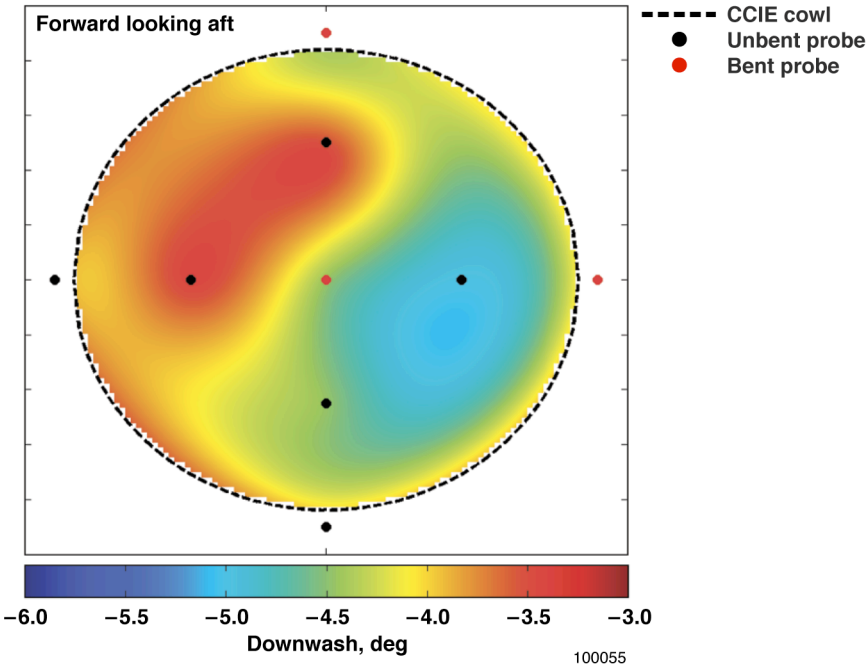

Flight 14a. Angle of attack.

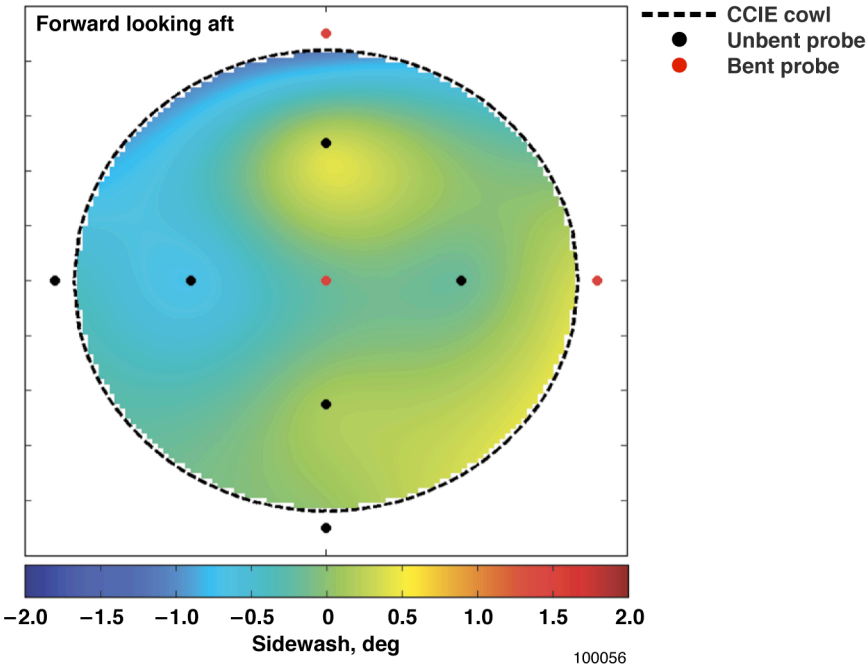

Flight 14b. Flank angle of attack.

Figure 14. Flow angularity contours at a free stream Mach number of 1.86 at 40,000 ft (flight 2).

2. Level Acceleration Results

Figure 15 shows the mean interface plane angle of attack and flank angle from both flights as a function of free-stream Mach number during an entire supersonic run. In figure 15a, the plot for flight 1 shows a linear relationship between mean local angle of attack and free-stream Mach number. Flight 2 displays a linear relationship as well, albeit with a different slope, up to approximately $M_\infty = 1.7$ where the

slope of the curve changes. The plots of mean local flank angle for both flights (fig. 15b) almost resemble mirror images of each other, and the angles were both within ± 0.5° for the entire supersonic run.

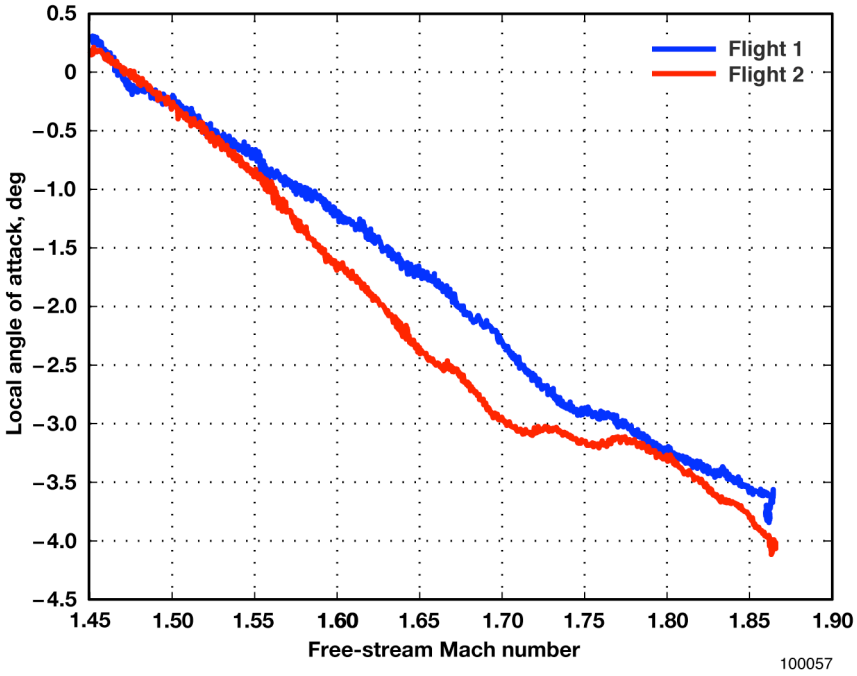

Figure 15a. Angle of attack.

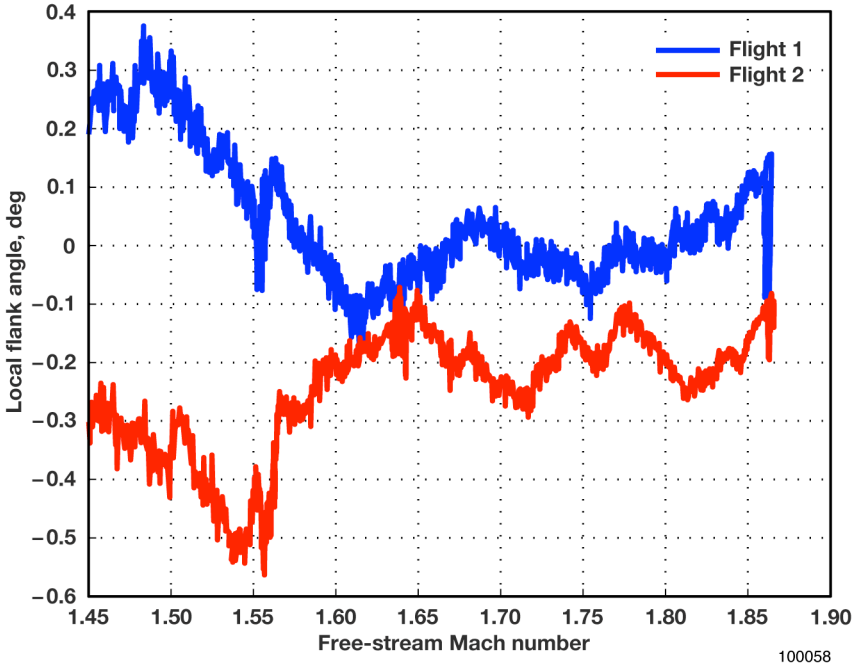

Figure 15b. Flank angle of attack.

Figure 15. Average flow angularity during the 40,000-ft supersonic acceleration runs.

3. Sources of Flow Angularity Discrepancies Observed Between Flights

An exhaustive analysis of the flight data was performed to try to determine the cause of the flow angularity discrepancies between flights. Several factors were determined to have had the potential to alter the local flow underneath the airplane. During flight 2, the airplane flew at roughly 0.25° of additional sideslip compared to flight 1. It was also noted that the free-stream temperature at altitude was 10°F cooler during flight 2. The colder, denser air allows the engines to operate more efficiently. The precise way in which this temperature difference affects inlet spillage is not completely understood, but it seems reasonable to believe that the spillage between the two flights was different, thus potentially altering the flow underneath the airplane. Lastly, two factors from the rake's calibration potentially affected the local flow measurements between the two flights as a result of the rake being rotated 180° for the second flight. As described in reference 5, each probe was not calibrated individually; instead, the rake was calibrated as a unit in a wind tunnel. Nonuniformities in the wind tunnel flow speed and direction had unquantifiable effects on the calibration of all of the probes, except possibly the center probe, because this probe was the only one that was fixed in space in the tunnel as the calibration data were obtained. Additionally, the calibration data that were obtained in the wind tunnel were insufficient to entirely eliminate misalignment bias between the rake and the flow in the tunnel.

IV. Concluding Remarks

The flow-field survey rake from the Rake Airflow Gage Experiment (RAGE), comprised of nine five-hole conical probes mounted in a cruciform configuration on the Propulsion Flight Test Fixture, was flown on the NASA Dryden F-15B research airplane in the latter half of 2009. The goal was to quantify the flow field underneath the F-15B airplane at the location of the aerodynamic interface plane of the Channeled Centerbody Inlet Experiment (CCIE), a novel supersonic inlet design scheduled for flight test at the National Aeronautics and Space Administration Dryden Flight Research Center in the near future. Steady-state test points were taken at pressure altitudes of 35,000, 40,000, and 45,000 ft over a range of free-stream Mach numbers, M_∞, up to 1.86. The local flow angularity, Mach number, total pressure distortion, and dynamic pressure were measured and correlated to airplane free-stream conditions.

Of primary importance to the RAGE was the determination of the free-stream Mach number that would produce a local Mach number, M_L, of 1.5 at the aerodynamic interface plane of the inlet. The data obtained from these flights suggest that a free-stream Mach number of 1.65 will produce $M_L = 1.5$. At this condition, the rake, already inclined 5° from horizontal, is not aligned with the flow, as there is an average of nearly 2° of downwash on the rake. Because axial flow is desired, it might be possible to fly the CCIE at a lower Mach number, perhaps $M_L = 1.48$, corresponding to $M_\infty = 1.56$. This condition would decrease the downwash to approximately 1°. A reduction in the local Mach number, however, also has the effect of reducing the local dynamic pressure, which is important, but not nearly as critical as the local Mach number to the performance of the inlet. Although the RAGE was conducted primarily in support of the CCIE, the data obtained in these flights have value to any future inlet experiments that utilize the Propulsion Flight Test Fixture.

References

1. Corda, Stephen, M. Jake Vachon, Nathan Palumbo, Corey Diebler, Ting Tseng, Anthony Ginn, and David Richwine, "The F-15B Propulsion Flight Test Fixture: A New Flight Facility for Propulsion Research," NASA/TM 2001-210395, 2005.

2. Vachon, Michael Jacob, Timothy R. Moes, and Stephen Corda, "Local Flow Conditions for Propulsion Experiments on the NASA F-15B Propulsion Flight Test Fixture," NASA/TM 2005-213670, 2005.

3. Palumbo, Nathan, Tim Moes, and M. Jake Vachon, "Initial Flight Tests of the NASA F-15B Propulsion Flight Test Fixture," AIAA 2002-4131, *Proceedings of the 38th AIAA/ASME/SAE/ASEE Joint Propulsion Conference and Exhibit*, Indianapolis, Indiana, July 7-10, 2002.

4. Weir, Lois J., Bobby W. Sanders, and Jake Vachon, "A New Design Concept for Supersonic Axisymmetric Inlets," AIAA 2002-3775, *Proceedings of the 38th AIAA/ASME/SAE/ASEE Joint Propulsion Conference and Exhibit*, Indianapolis, Indiana, July 7-10, 2002.

5. Flynn, Darin C., Nalin A. Ratnayake, and Michael Frederick, "Design and Calibration of a Flowfield Survey Rake for Inlet Flight Research," AIAA 2009-1484, *Proceedings of the 47th AIAA Aerospace Sciences Meeting Including The New Horizons Forum and Aerospace Exposition*, Orlando, Florida, January 5-8, 2009.

6. Miller, K. J., J. C. Sisco, B. L. Austin, Jr., T. N. Martin III, W. E. Anderson, and Nathan M. Palumbo, "Direct-Connect Simultaneously Mixing and Combusting Ducted Rocket Build and Test," 2003-0390FB, *39th JANNAF Combustion Subcommittee Meeting*, Colorado Springs, Colorado, December 1–5, 2003.

7. Gracey, William, "Measurement of Aircraft Speed and Altitude," NASA RP-1046, 1980.

8. Huston, Wilber B., "Accuracy of Airspeed Measurements and Flight Calibration Procedures," NACA TR-919, 1948.